communications physics

ARTICLE

https://doi.org/10.1038/s42005-022-00912-4 OPEN

Universal constraint on nonlinear population dynamics

Kyosuke Adachi[1,2✉], Ryosuke Iritani[2,3] & Ryusuke Hamazaki[2,4]

Ecological and evolutionary processes show various population dynamics depending on internal interactions and environmental changes. While crucial in predicting biological processes, discovering general relations for such nonlinear dynamics has remained a challenge. Here, we derive a universal information-theoretical constraint on a broad class of nonlinear dynamical systems represented as population dynamics. The constraint is interpreted as a generalization of Fisher's fundamental theorem of natural selection. Furthermore, the constraint indicates nontrivial bounds for the speed of critical relaxation around bifurcation points, which we argue are universally determined only by the type of bifurcation. Our theory is verified for an evolutionary model and an epidemiological model, which exhibit the transcritical bifurcation, as well as for an ecological model, which undergoes limit-cycle oscillation. This work paves a way to predict biological dynamics in light of information theory, by providing fundamental relations in nonequilibrium statistical mechanics of nonlinear systems.

[1] Nonequilibrium Physics of Living Matter RIKEN Hakubi Research Team, RIKEN Center for Biosystems Dynamics Research (BDR), 2-2-3 Minatojima-minamimachi, Chuo-ku, Kobe 650-0047, Japan. [2] RIKEN Interdisciplinary Theoretical and Mathematical Sciences Program (iTHEMS), 2-1 Hirosawa, Wako 351-0198, Japan. [3] Department of Biological Sciences, Graduate School of Science, University of Tokyo, 7-3-1 Hongo, Bunkyo-ku, Tokyo 113-0033, Japan. [4] Nonequilibrium Quantum Statistical Mechanics RIKEN Hakubi Research Team, RIKEN Cluster for Pioneering Research (CPR), 2-1 Hirosawa, Wako 351-0198, Japan. ✉email: kyosuke.adachi@riken.jp

Nonlinear dynamics appears in a variety of fields, including classical mechanics, chemical reaction systems, and population biology, to name a few[1]. Nonlinearity can trigger complex temporal and spatial patterns and even chaotic behaviors, making it challenging to find universal relations within the properties of dynamics. In particular, slight perturbations in external parameters can result in qualitative changes in the dynamical property through a bifurcation such as the Hopf bifurcation, where self-sustained oscillation emerges. It is of pivotal importance to explore universal relations shared by a broad class of dynamical phenomena with nonlinearity.

Ecological and evolutionary processes often exhibit nonlinear population dynamics[2,3] such as temporal oscillation in population sizes and irreversible extinction of certain species[4]. Typical biological systems consist of identifiable units such as genotypes and species (called "types" in this paper), and intra-type and inter-type interactions cause nonlinear dynamics[2,4]. Besides interactions, type-dependent growth rates determined by natural selection lead to nonlinear dynamics of the proportions of each type. In evolutionary theory, Fisher's fundamental theorem of natural selection[5,6] establishes a simple relation between the variance of the growth rate and the temporal increase in the average growth rate. The theorem has been extended to evolutionary models with mutation[7,8] and ecological models[9].

Bifurcations and associated critical dynamics play significant roles in biological processes[10]. In ecological[11,12] and epidemiological[13] systems, critical slowing down around bifurcation points has been discussed as an early warning signal for catastrophic shifts. In evolutionary systems, bifurcation points can appear as critical mutation rates beyond which heredity does not persist[14,15], and the self-organized criticality has also been discussed as a possible mechanism of mass extinction of species[16]. Since such critical dynamics reflects instabilities behind nonlinear systems[17], fundamental relations near bifurcation points are crucial in predicting dramatic changes in ecological and evolutionary processes.

We here derive a general constraint on nonlinear population dynamics by extending the formulation developed for stochastic processes[18,19] to nonlinear dynamical systems. In particular, Fisher's fundamental theorem of natural selection is a special case of the constraint. As a unique consequence of the constraint, we show that the critical scaling exponents of speeds near the bifurcation point should have nontrivial bounds that are universally determined by the type of bifurcation. We verify our theory for an evolutionary model with mutation and the susceptible-infected-recovered (SIR) model with birth and death, which show the transcritical bifurcation, as well as for the competitive Lotka–Volterra model, which undergoes limit-cycle oscillation.

Results

Constraint on general population dynamics. We consider a general population dynamics described by

$$\partial_t N_i = F_i(N_1, ..., N_L), \tag{1}$$

where i is the label for each type, L is the total number of types, and $N_i(t)$ is the density of type i at time t. If there are interactions between types, $F_i(N_1, \ldots, N_L)$ is generally a nonlinear function. Defining the proportion $P := \{P_i\}_{i=1}^L := \{N_i/N_{\rm tot}\}_{i=1}^L$ with the total population density $N_{\rm tot} := \sum_{i=1}^L N_i$, we obtain equations for P_i and $N_{\rm tot}$ as

$$\partial_t P_i = \frac{F_i(N_{\rm tot}P_1, ..., N_{\rm tot}P_L)}{N_{\rm tot}} - P_i \sum_{j=1}^{L} \frac{F_j(N_{\rm tot}P_1, ..., N_{\rm tot}P_L)}{N_{\rm tot}} \tag{2}$$

and $\partial_t N_{\rm tot} = \sum_{i=1}^L F_i(N_{\rm tot}P_1, ..., N_{\rm tot}P_L)$, respectively. Even if $F_i(N_1, \ldots, N_L)$ is a linear function for all i, Eq. (2) can be a nonlinear equation, and bifurcations can occur as we discuss later.

Applying the Cauchy-Schwarz inequality to the Price equation[20,21], which is derived from the conservation of the total proportion ($\sum_{i=1}^L P_i = 1$), we obtain the speed-limit inequality (Supplementary Method 1):

$$v_A \le v_{\rm lim} := \sqrt{I_{\rm F}} := \sqrt{\left\langle (\partial_t P/P)^2 \right\rangle}. \tag{3}$$

Note that an inequality whose expression is the same as Eq. (3) has been discussed for stochastic processes[18,19], and the relation to the Price equation has been pointed out[21]. Here, we define the Fisher information $I_{\rm F}$[22,23] and the speed $v_A := |\partial_t \langle A\rangle - \langle \partial_t A\rangle|/\Delta A$, which characterizes the temporal change rate of a type-dependent quantity $A := \{A_i\}_{i=1}^L$ that can depend on time in general [Supplementary Method 1, Fig. 1(a)]. Also, the average and standard deviation are defined as $\langle A\rangle := \sum_{i=1}^L P_i A_i$ and $\Delta A := (\langle A^2\rangle - \langle A\rangle^2)^{1/2}$, respectively. The inequality [Eq. (3)] provides a universal upper bound on the speed of population dynamics, independent of the choice of quantity A [Fig. 1(b)]. We stress that Eq. (3) applies to nonlinear dynamics though the expression is equivalent to that for Markov processes[18,19], where the probability distribution follows linear dynamics. For example, $v_{\rm lim}$ in Eq. (3) can be a non-monotonic function of time, in contrast to Markovian relaxation processes, where $v_{\rm lim}$ decays monotonically[18]. Note that Eq. (3) is different from the previously obtained speed-limit inequalities in nonlinear systems[24,25], which have been discussed mainly for chemical reaction networks. Following Nicholson et al.[19], we can interpret Eq. (3) as the uncertainty relation between the timescale of dynamical quantities (${v_A}^{-1}$) and the information of dynamics ($\sqrt{I_{\rm F}}$).

Relation to Fisher's fundamental theorem. Our general constraint includes Fisher's fundamental theorem as a special case when applied to an evolutionary model with natural selection. We take $F_i = s_i N_i$ in Eq. (1), where $s_i > 0$ is the type-dependent growth rate. In such systems, Fisher's fundamental theorem of natural selection asserts that the increase in the average growth rate is equal to the variance of the growth rate[5,7], i.e., $\partial_t\langle s\rangle = (\Delta s)^2$. As shown in Supplementary Method 2, we find that Fisher's fundamental theorem is a special case of Eq. (3), $v_s = v_{\rm lim}$. Note that $v_{\rm lim}$ in Eq. (3) is equivalent to Crow's index of opportunity for selection, which provides an empirical estimate of the maximum strength of natural selection acting on a given population[26,27].

Furthermore, even when the growth rate depends on time and densities, we show that an extended version of the fundamental theorem[6,9] is a special case of Eq. (3), where the equality in Eq. (3) is satisfied (Supplementary Method 2). Our result therefore covers a variety of previous results established in population biology in light of information theory and statistical physics. For more general dynamics with mutation, the speed-limit inequality [Eq. (3)] is satisfied for any quantity A, including the growth rate s, and thus regarded as a generalization of the fundamental theorem. For instance, if we take the typical length of type i as A_i (e.g., length of bacteria for several types of mutants), the average length can potentially change more quickly as the variance of the length is larger, according to Eq. (3). Note that other types of extensions of the fundamental theorem to evolutionary models with mutation has been formulated[7,8].

Speed limit for evolutionary dynamics. We next consider another evolutionary model with natural selection and mutation [Fig. 1(d)] by taking $F_i = s_i N_i + \sum_{j=1}^L m_{ij} N_j$ in Eq. (1)[14,28]. Here,

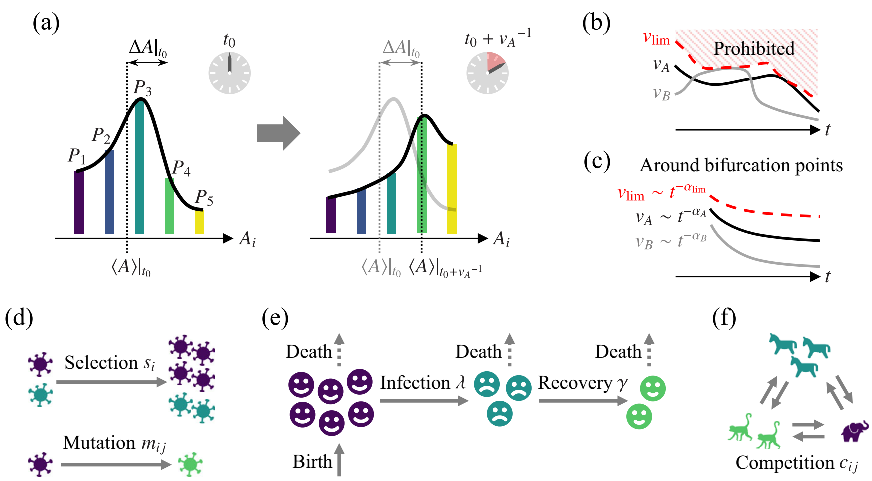

Fig. 1 Speed-limit inequality in ecological and evolutionary dynamics. a For a quantity A, the inverse of the speed, $v_A{}^{-1}$, represents the time required for the instantaneous average $\langle A\rangle$ to change by the instantaneous standard deviation ΔA. The proportion of type i (density of type i divided by the total density), P_i, changes as the time $v_A{}^{-1}$ passes. In **a**, we assume $A_1 < A_2 < A_3 < A_4 < A_5$ without loss of generality, and the black and gray lines are the guides for the eye. **b** For a quantity A at any time t, any speed (black solid line) faster than $v_{\rm lim}$ (red dashed line) is prohibited. This applies to any quantity, as illustrated by the gray solid line for another quantity B. **c** Around bifurcation points, the speed for a quantity A (black solid line) and the speed limit (red dashed line) show power-law decays as $v_A \sim t^{-\alpha_A}$ and $v_{\rm lim} \sim t^{-\alpha_{\rm lim}}$ with a constraint $\alpha_A \geq \alpha_{\rm lim}$, where $\alpha_{\rm lim}$ is universally determined by the bifurcation type. This applies to any quantity, as illustrated by the gray solid line for another quantity B. In this study, we mainly consider three models: **d** the evolutionary model with natural selection and mutation (with growth rate s_i and mutation rate m_{ij}), **e** the epidemiological model called susceptible-infected-recovered (SIR) model (with birth and death rates 1, infection rate λ, and recovery rate γ), and **f** the ecological model called competitive Lotka–Volterra model (with competitive interaction c_{ij}).

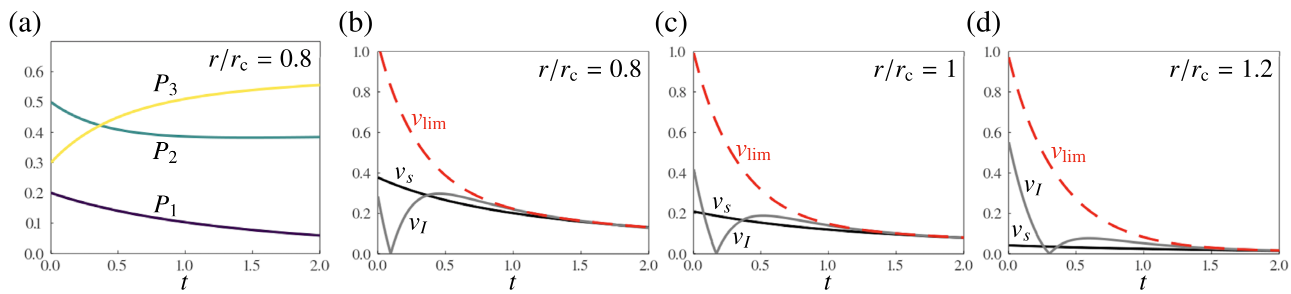

Fig. 2 Speed limit for the evolutionary dynamics with natural selection and mutation. a Typical dependence on time (t) of the proportion of type i (density of type i divided by the total density), P_i, for $r/r_{\rm c} = 0.8$. Here, r is the growth rate for type 1 relative to that for type 2 or 3, and $r_{\rm c}$ is the value of r at the transcritical bifurcation point. **b–d** The speed-limit inequality [Eq. (3)] holds, regardless of the parameters ($r/r_{\rm c}$) and quantities (growth rate s or diversity I). The speed of the growth rate v_s (black solid line) and that of change in diversity v_I (gray solid line) are compared with the speed limit $v_{\rm lim}$ (red dashed line) for **b** $r/r_{\rm c} = 0.8$, **c** $r/r_{\rm c} = 1$, and **d** $r/r_{\rm c} = 1.2$. See Supplementary Method 3 for the other parameters used.

$s_i > 0$ is the growth rate and $m_{ij} \geq 0$ $(i \neq j)$ is the mutation rate from type j to i. To demonstrate the inequality [Eq. (3)], we take $L = 3$ with $s_2 = s_3 = \bar{s}$ and examine a situation where type 1 will survive (become extinct) after a long time if the growth rate $s_1 = \bar{s} + r$ is larger (smaller) than a critical value $\bar{s} + r_{\rm c}$ (Supplementary Method 3). The extinction transition at $r = r_{\rm c}$ corresponds to the transcritical bifurcation[1].

Figure 2(a) shows typical time dependence of the proportion P_i. As shown in Fig. 2(b–d), regardless of the value of $r/r_{\rm c}$, the speed of the growth rate v_s (black solid lines) is bounded by the speed limit $v_{\rm lim}$ (red dashed lines), which verifies Eq. (3). To confirm the generality of Eq. (3), we introduce the Shannon entropy $I_{\rm S} := \langle I\rangle$ with $I := \{I_i\}_{i=1}^{L} := \{-\ln P_i\}_{i=1}^{L}$ [23] as the (logarithm of) diversity of population (see Supplementary Fig. 1 for typical time dependence of $I_{\rm S}$). We show that the speed of change in diversity, v_I (gray solid lines), is also bounded by $v_{\rm lim}$.

Universal constraint around transcritical bifurcation point. Let us examine a consequence of the speed limit at the transcritical bifurcation point ($r = r_{\rm c}$), where an observable A typically exhibits critical slowing down[10,13] with a power-law decay of the speed, $v_A \sim t^{-\alpha_A}$. While α_A can vary for different A, the inequality [Eq. (3)] indicates that α_A is bounded by a universal factor $\alpha_{\rm lim}$ determined by the Fisher information [Fig. 1(c)]. Note that the power-law decrease in the Fisher information has also been discussed for the transient dynamics in nonlinear oscillator models[29]. In the evolutionary model with natural selection and mutation, we find $P_1 \sim t^{-1}$ (Supplementary Method 3) and thus

$$v_{\rm lim} \sim \sqrt{(\partial_t P_1)^2/P_1} \sim t^{-\alpha_{\rm lim}^{\rm TC}} \tag{4}$$

with $\alpha_{\rm lim}^{\rm TC} = 3/2$. Then, we have

$$\alpha_A \geq \alpha_{\rm lim}^{\rm TC} = 3/2 \tag{5}$$

for arbitrary A in this process.

In addition, if the parameter is slightly off the bifurcation point, the system can exhibit dynamical scaling, in a manner similar to critical phenomena[30–32]. Assuming that the relaxation times of the speed and the speed limit diverge at the bifurcation point as

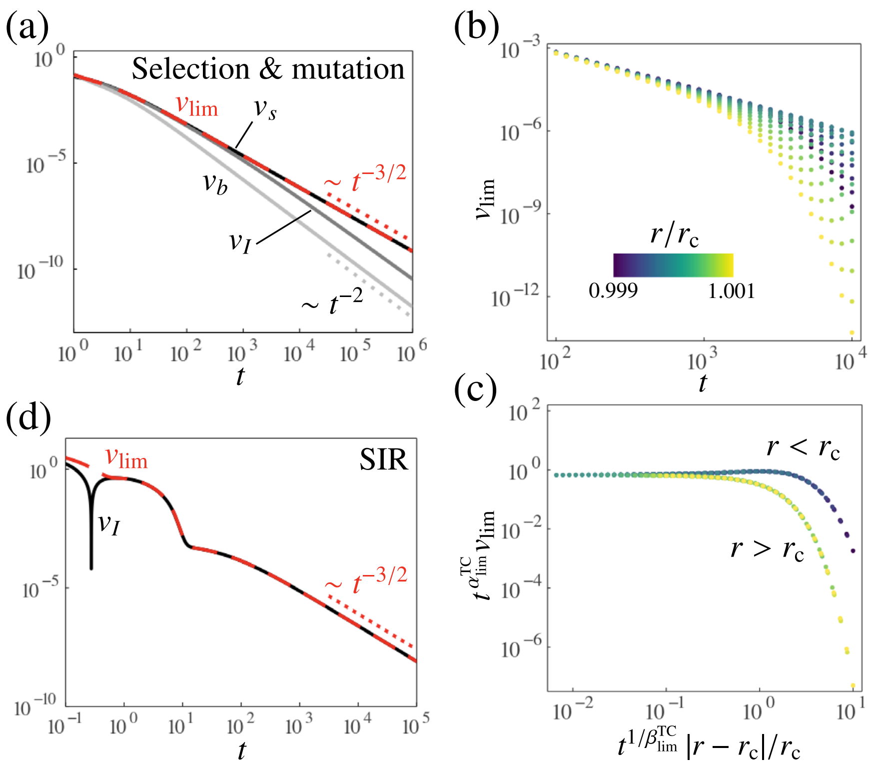

Fig. 3 Universal bounds for the critical scaling exponents at the transcritical bifurcation. **a** Power-law decay of the speed of the growth rate (v_s, black solid line), the speed of the change in diversity (v_I, dark-gray solid line), the speed of the type index (v_b, light-gray solid line), and the speed limit ($v_{\rm lim}$, red dashed line) at the transcritical bifurcation point ($r = r_c$) of the evolutionary model with selection and mutation. Here, t is the time, r is the growth rate for type 1 relative to that for type 2 or 3, and r_c is the value of r at the transcritical bifurcation point. The asymptotic forms ($v_{\rm lim} \sim t^{-3/2}$ and $v_b \sim t^{-2}$) are shown with dotted lines. **b** Time and parameter dependence of $v_{\rm lim}$ and **c** the corresponding scaling plot near the bifurcation point ($0.999 \le r/r_c \le 1.001$). The exponents at the transcritical (TC) point are given as $\alpha_{\rm lim}^{\rm TC} = 3/2$ [see Eq. (4)] and $\beta_{\rm lim}^{\rm TC} = 1$ [see Eq. (7)]. **d** Power-law decay of v_I (black solid line) and $v_{\rm lim}$ (red dashed line) at the transcritical bifurcation point of the susceptible-infected-recovered (SIR) model. The asymptotic form ($v_{\rm lim} \sim t^{-3/2}$) is shown with a dotted line. For **a**–**c**, we use the same parameters as those for Fig. 2. See Supplementary Method 4 for the parameters used for **d**.

$\sim |r - r_c|^{-\beta_A}$ and $\sim |r - r_c|^{-\beta_{\rm lim}^{\rm TC}}$, respectively, we obtain the dynamical scaling laws as

$$v_A(r - r_c, t) \simeq t^{-\alpha_A} f_A^{\pm}(t^{1/\beta_A}|r - r_c|), \tag{6}$$

$$v_{\rm lim}(r - r_c, t) \simeq t^{-\alpha_{\rm lim}^{\rm TC}} f_{\rm lim}^{\pm}(t^{1/\beta_{\rm lim}^{\rm TC}}|r - r_c|), \tag{7}$$

where f_A^+ and $f_{\rm lim}^+$ (f_A^- and $f_{\rm lim}^-$) are scaling functions for $r - r_c > 0$ (< 0). Combining the inequality [Eq. (3)] and the scaling laws [Eqs. (6) and (7)], we derive another constraint on the exponents as $\beta_A \le \beta_{\rm lim}^{\rm TC}$ (Supplementary Method 3). In the numerical simulations, we have only found the case with $\beta_A = \beta_{\rm lim}^{\rm TC}$ (see below), which suggests that the diverging relaxation time of any speed should be proportional to the relaxation time of a single quantity (i.e., P_1 in the present model) in a similar way to critical phenomena[30,31].

To confirm the above argument, we demonstrate the long-time relaxation of $v_{\rm lim}$, v_s, v_I, and a speed v_b for the type index $b := \{b_i\}_{i=1}^L := \{i\}_{i=1}^L$ at the bifurcation point ($r = r_c$) [Fig. 3(a)]. We find $v_{\rm lim} \sim t^{-3/2}$ [red dotted line in Fig. 3(a)], which is consistent with Eq. (4). We also obtain $v_s \sim t^{-3/2}$, $v_I \sim t^{-2} \ln t$, and $v_b \sim t^{-2}$ (see Supplementary Method 3 for the derivation), and the corresponding exponents are $\alpha_s = 3/2$, $\alpha_I = 2$ (neglecting the logarithmic dependence), and $\alpha_b = 2$, which indeed satisfy the inequality [Eq. (5)]. Moreover, slightly off the bifurcation point, we find the expected scaling laws [Eq. (6) and Eq. (7)] of v_s, v_b (Supplementary Fig. 2), and $v_{\rm lim}$ [Fig. 3(b) and (c)] with $\beta_s = \beta_b = \beta_{\rm lim}^{\rm TC} = 1$.

Beyond specific dynamics, we conjecture that the exponents for the power-law decay of the speeds at the bifurcation point in population dynamics are bounded by a universal constant $\alpha_{\rm lim}$ that only depends on the type of bifurcation. Similarly, the exponent $\beta_{\rm lim}$ is also conjectured to be determined by the bifurcation type. These conjectures are plausible because critical properties associated with the bifurcation can be essentially described by the normal form for each bifurcation type[1,32]. This universal constraint on the exponents is a unique property of nonlinear dynamics, in contrast to the previous works on speed limits for linear dynamics[18,19].

As a primary example, the inequality [Eq. (5)] can be generally applied to nonlinear dynamics that undergoes an extinction transition through the transcritical bifurcation. We consider the SIR model with birth and death [Fig. 1(e)], where N_1, N_2, and N_3 are the densities of susceptible, infected, and recovered individuals, respectively[33] (Supplementary Method 4). This model is genuinely nonlinear in that $F_i(N_1, N_2, N_3)$ in Eq. (1) is a nonlinear function. In this model, the transcritical bifurcation occurs as an extinction transition of the infected and recovered individuals, i.e., a transition between the disease-free and endemic states, and the critical slowing down occurs ($P_2 \sim P_3 \sim t^{-1}$) at the bifurcation point (Supplementary Method 4). In Supplementary Fig. 3, we show typical time dependence of the proportion at the bifurcation point. We find that the speed of change in diversity v_I and the speed limit $v_{\rm lim}$ follow the same power-law decay as $v_I \sim v_{\rm lim} \sim t^{-3/2}$ [Fig. 3(d)], satisfying the Eqs. (4) and (5).

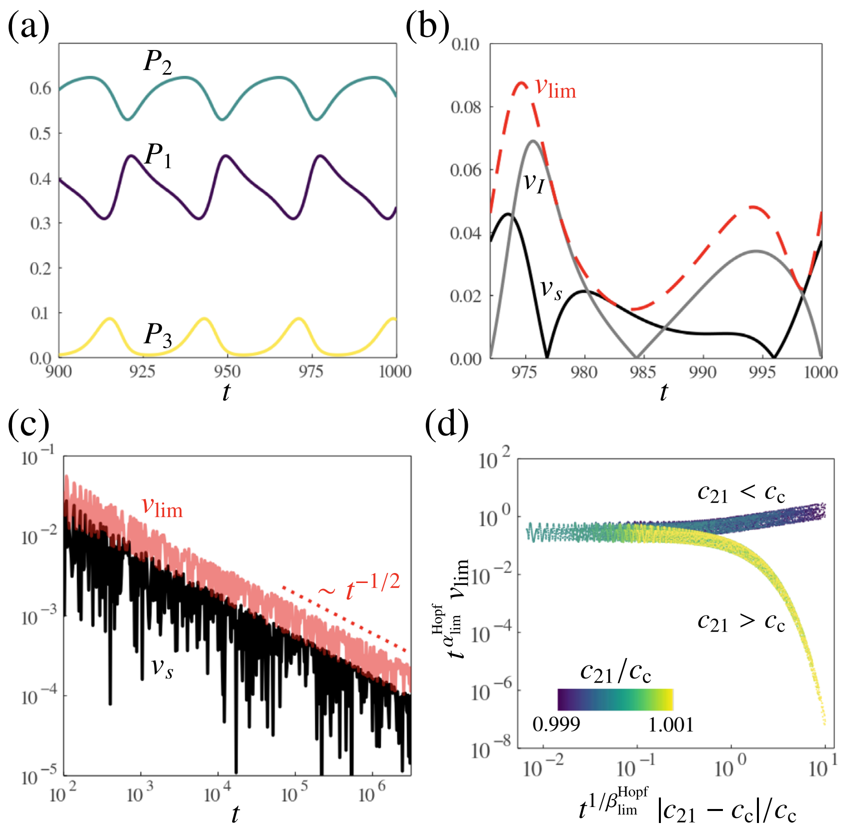

Fig. 4 Universal bounds for the critical scaling exponents at the supercritical Hopf bifurcation. Limit-cycle oscillation of **a** the proportion of type i (density of type i divided by the total density), P_i, and **b** the speed of the growth rate (v_s, black solid line), the speed of change in diversity (v_I, gray solid line), and the speed limit ($v_{\rm lim}$, red dashed line) as a function of time t in the competitive Lotka–Volterra model. **c** Power-law decay of $v_{\rm lim}$ (red line), compared with v_s (black line) at the Hopf bifurcation point. The asymptotic form of the amplitude relaxation ($v_{\rm lim} \sim t^{-1/2}$) is shown with a dotted line. The curves are rattling since the number of plotted points is finite; similarly to **b**, v_s oscillates between zero and nonzero values, while $v_{\rm lim}$ stays nonzero. **d** Scaling plot of the time and interaction dependence of $v_{\rm lim}$ near the bifurcation point ($0.999 \le c_{21}/c_{\rm c} \le 1.001$). The limit cycle appears for $c_{21} < c_{\rm c}$, while the steady-state coexistence of three types appears for $c_{21} \ge c_{\rm c}$, where c_{21} is the competitive interaction strength from type 1 to type 2, and $c_{\rm c}$ is the value of c_{21} at the Hopf bifurcation point (Supplementary Method 6). The exponents are given as $\alpha_{\rm lim}^{\rm Hopf} = 1/2$ and $\beta_{\rm lim}^{\rm Hopf} = 1$. See Supplementary Method 6 for the parameters used.

Universal constraint around Hopf bifurcation point. To verify our conjecture for other types of bifurcations, we focus on the Hopf bifurcation, at which a limit cycle starts to appear[1]. According to the normal form of the supercritical Hopf bifurcation, the deviation from the steady state decays with oscillation as $\sim t^{-1/2}\cos\omega t$ at the bifurcation point (Supplementary Method 5). Thus, for population dynamics undergoing the supercritical Hopf bifurcation, the proportion follows $P_i \sim \text{const.} + t^{-1/2}\cos\omega t$, and the speed limit decays as

$$v_{\rm lim} = \sqrt{\sum_{i=1}^{L} (\partial_t P_i)^2/P_i} \sim t^{-\alpha_{\rm lim}^{\rm Hopf}}, \tag{8}$$

with $\alpha_{\rm lim}^{\rm Hopf} = 1/2$, where we only consider the amplitude relaxation by neglecting the oscillatory component. Correspondingly, if we assume a power-law decay of the speed amplitude as $v_A \sim t^{-\alpha_A}$, α_A should satisfy

$$\alpha_A \ge \alpha_{\rm lim}^{\rm Hopf} = 1/2. \tag{9}$$

As an ecological model that undergoes the supercritical Hopf bifurcation, we consider the competitive Lotka–Volterra model [Fig. 1(f)] by taking $F_i = s_i N_i - \sum_{j=1}^{L} c_{ij} N_i N_j$ in Eq. (1)[4,34]. Here, s_i is the growth rate, $c_{ij} > 0$ represents the competitive interaction between type i and j, and these parameters are set around the Hopf bifurcation (Supplementary Method 6).

We first show typical limit-cycle oscillation of the proportion [Fig. 4(a)]. Comparing v_s, v_I, and $v_{\rm lim}$ within a single period [Fig. 4(b)], we confirm that the inequality [Eq. (3)] holds even when the limit cycle appears. By tuning the parameters to the Hopf bifurcation point, we numerically find the power-law decay of the speed amplitudes[35] as $v_s \sim v_I \sim v_{\rm lim} \sim t^{-1/2}$ [Fig. 4(c) and Supplementary Fig. 4], verifying Eqs. (8) and (9). Then, changing the parameters slightly off the bifurcation point, we find that the counterparts of the scaling laws [Eqs. (6) and (7)] hold for the speed amplitudes [Fig. 4(d) and Supplementary Fig. 5] with $\beta_s = \beta_I = \beta_{\rm lim}^{\rm Hopf} = 1$.

Conclusion

We have illustrated the applications of the dynamical constraint [Eq. (3)] to ecological and evolutionary models. Focusing on the bifurcation unique to nonlinear dynamics, we have argued that the exponents of speeds at critical slowing down have the universal bounds that depend only on the bifurcation type. In particular, for the transcritical and supercritical Hopf bifurcations, we have confirmed the theoretically obtained Eqs. (4)–(9) using numerical simulations. Similar formulae are obtained for other bifurcations, e.g., $\alpha_A \ge \alpha_{\rm lim}^{\rm SN} = 2$ for the saddle-node bifurcation (Supplementary Method 7), which appears in population dynamics[11,12,17].

Considering the probability[18,19] instead of the proportion, we may extend our argument to critical phenomena in many-body stochastic systems, which can express nonequilibrium phenomena different from ecological and evolutionary dynamics. For instance, lattice gas models[30], the contact process[31], and biological systems such as swarms[36] are potentially subject to constraints corresponding to Eqs (5) or (9) with possibly irrational lower bounds.

The methodologies of ecology and evolution have been developed almost independently[37]. However, ecological and evolutionary dynamics may not be separable in some situations. For example, rapid evolution can occur on the same timescale as that of ecological processes when there are drastic environmental changes[37]. General relations such as Eq. (3) will be useful in quantitative understanding of even inseparable eco-evolutionary dynamics.

Data availability

All the data that support the plots and the other findings of this study are available from the corresponding author upon reasonable request.

Code availability

All the computational codes that were used to generate the data presented in this study are available from the corresponding author upon reasonable request.

Received: 23 January 2022; Accepted: 11 May 2022;
Published online: 01 June 2022

References

1. Strogatz, S. H. *Nonlinear Dynamics and Chaos with Student Solutions Manual: With Applications to Physics, Biology, Chemistry, and Engineering* (CRC Press, 2018).
2. Levine, J. M., Bascompte, J., Adler, P. B. & Allesina, S. Beyond pairwise mechanisms of species coexistence in complex communities. *Nature* **546**, 56–64 (2017).
3. Hastings, A. et al. Transient phenomena in ecology. *Science* **361**, eaat6412 (2018).
4. Hofbauer, J. & Sigmund, K. *Evolutionary Games and Population Dynamics* (Cambridge University Press, 1998).
5. Li, C. C. Fundamental theorem of natural selection. *Nature* **214**, 505–506 (1967).
6. Edwards, A. W. F. The fundamental theorem of natural selection. *Biol. Rev.* **69**, 443–474 (1994).
7. Basener, W. F. & Sanford, J. C. The fundamental theorem of natural selection with mutations. *J. Math. Biol.* **76**, 1589–1622 (2018).
8. Basener, W., Cordova, S., Hössjer, O. & Sanford, J. Dynamical systems and fitness maximization in evolutionary biology. In Sriraman, B. (ed.) *Handbook of the Mathematics of the Arts and Sciences*, 1–72 (Springer International Publishing, Cham, 2020). https://doi.org/10.1007/978-3-319-70658-0_121-1.
9. Baez, J. C. The fundamental theorem of natural selection. *Entropy* **23**, 1436 (2021).
10. Muñoz, M. A. Colloquium: Criticality and dynamical scaling in living systems. *Rev. Mod. Phys.* **90**, 031001 (2018).
11. Veraart, A. J. et al. Recovery rates reflect distance to a tipping point in a living system. *Nature* **481**, 357–359 (2012).
12. Dai, L., Vorselen, D., Korolev, K. S. & Gore, J. Generic indicators for loss of resilience before a tipping point leading to population collapse. *Science* **336**, 1175–1177 (2012).
13. Drake, J. M. et al. The statistics of epidemic transitions. *PLOS Comput. Biol.* **15**, 1–14 (2019).
14. Bull, J. J., Meyers, L. A. & Lachmann, M. Quasispecies made simple. *PLOS Comput. Biol.* **1**, 1–11 (2005).
15. Solé, R., Sardanyés, J. & Elena, S. F. Phase transitions in virology. *Rep. Prog. Phys.* **84**, 115901 (2021).
16. Sneppen, K., Bak, P., Flyvbjerg, H. & Jensen, M. H. Evolution as a self-organized critical phenomenon. *Proc. Natl Acad. Sci. USA* **92**, 5209–5213 (1995).
17. Scheffer, M., Carpenter, S. R., Dakos, V. & van Nes, E. H. Generic indicators of ecological resilience: Inferring the chance of a critical transition. *Annu. Rev. Ecol. Evol. Syst.* **46**, 145–167 (2015).
18. Ito, S. & Dechant, A. Stochastic time evolution, information geometry, and the cramér-rao bound. *Phys. Rev. X* **10**, 021056 (2020).
19. Nicholson, S. B., García-Pintos, L. P., del Campo, A. & Green, J. R. Time–information uncertainty relations in thermodynamics. *Nat. Phys.* **16**, 1211–1215 (2020).
20. Price, G. R. Extension of covariance selection mathematics. *Ann. Hum. Genet.* **35**, 485–490 (1972).
21. Frank, S. A. & Bruggeman, F. J. The fundamental equations of change in statistical ensembles and biological populations. *Entropy* **22**, 1395 (2020).
22. Frank, S. A. Natural selection maximizes fisher information. *J. Evol. Biol.* **22**, 231–244 (2009).
23. Cover, T. M. & Thomas, J. A. *Elements of Information Theory* (Wiley, 2012).
24. Yoshimura, K. & Ito, S. Information geometric inequalities of chemical thermodynamics. *Phys. Rev. Res.* **3**, 013175 (2021).
25. Yoshimura, K. & Ito, S. Thermodynamic uncertainty relation and thermodynamic speed limit in deterministic chemical reaction networks. *Phys. Rev. Lett.* **127**, 160601 (2021).
26. Crow, J. F. Some possibilities for measuring selection intensities in man. *Hum. Biol.* **61**, 763–775 (1989).
27. Waples, R. S. An estimator of the opportunity for selection that is independent of mean fitness. *Evolution* **74**, 1942–1953 (2020).
28. Domingo, E. & Perales, C. Viral quasispecies. *PLoS Genet.* **15**, 1–20 (2019).
29. Hollerbach, R., Dimanche, D. & Kim, E.-j. Information geometry of nonlinear stochastic systems. *Entropy* **20**, 550 (2018).
30. Schmittmann, B. & Zia, R. Statistical mechanics of driven diffusive systems, vol. 17 of *Phase Transitions and Critical Phenomena* (Academic Press, 1995). https://www.sciencedirect.com/science/article/pii/S1062790106800145.
31. Henkel, M., Hinrichsen, H. & Lübeck, S. *Non-Equilibrium Phase Transitions, Vol. I: Absorbing Phase Transitions* (Springer, 2008).
32. Corral, Á., Sardanyés, J. & Alsedà, L. Finite-time scaling in local bifurcations. *Sci. Rep.* **8**, 11783 (2018).
33. Kretzschmar, M. & Wallinga, J. *Mathematical Models in Infectious Disease Epidemiology*, 209–221 (Springer New York, 2010). https://doi.org/10.1007/978-0-387-93835-6_12.
34. Zeeman, M. L. Hopf bifurcations in competitive three-dimensional lotka-volterra systems. *Dyn. Stab. Syst.* **8**, 189–216 (1993).
35. Strizhak, P. & Menzinger, M. Slow passage through a supercritical hopf bifurcation: Time-delayed response in the Belousov–Zhabotinsky reaction in a batch reactor. *J. Chem. Phys.* **105**, 10905–10910 (1996).
36. Cavagna, A. et al. Dynamic scaling in natural swarms. *Nat. Phys.* **13**, 914–918 (2017).
37. Bell, G. Evolutionary rescue. *Annu. Rev. Ecol. Evol. Syst.* **48**, 605–627 (2017).

Acknowledgements

We thank the Information Theory Study Group and Biology Seminar members in RIKEN iTHEMS and Kyogo Kawaguchi for scientific discussions. We also thank Yohsuke T. Fukai, Takashi Okada, and Takaki Yamamoto for helpful comments. This work was supported by JSPS KAKENHI Grant Numbers JP20K14435 (to K.A.), JP19K22457, JP19K23768, JP20K15882 (to R.I.), and RIKEN iTHEMS.

Author contributions

K.A. and R.I. conceived the project. K.A., R.I., and R.H. performed the analytic calculations. K.A. performed the simulations and made all the plots. K.A. drafted the initial version of the paper. K.A., R.I., and R.H. discussed the results and wrote the paper.

Competing interests

The authors declare no competing interests.

Additional information

Supplementary information The online version contains supplementary material available at https://doi.org/10.1038/s42005-022-00912-4.

Correspondence and requests for materials should be addressed to Kyosuke Adachi.

Peer review information *Communications Physics* thanks Andreas Dechant and the other, anonymous, reviewer(s) for their contribution to the peer review of this work. Peer reviewer reports are available.